ECWS-9
2025
Conference
The 9th International Electronic Conference on Water Sciences
11–14 November 2025 | Online
MDPI

Effects of Rayleigh number on thermal siphons in Triangular Water Bodies

Vassilios PAPAIOANNOU[1], Panagiotis PRINOS[2]
[1] Senior Researcher, Information Technologies Institute/ CERTH, Thessaloniki, Greece, email: vaspapa@iti.gr
[2] Emeritus Professor, Dept. of Civil Eng./ AUTh, Thessaloniki, Greece, email: prinosp@civil.auth.gr

INTRODUCTION & AIM

Natural convection in enclosed or semi-enclosed water bodies (e.g., lakes, reservoirs) drives vertical and horizontal heat and momentum exchange. Surface cooling creates density differences between shallow and deep regions, generating thermal siphons [1], [2]. In triangular or sloping-bottom basins, nearshore areas cool faster, triggering downslope gravity currents and upwelling in deeper zones, affecting mixing, stratification, and heat distribution [3]. Most studies focus on low to moderate Rayleigh numbers (*Ra*) [4], while high-*Ra* turbulent flows remain less explored.

This study aims to:
1. Examine thermal siphon formation under surface cooling in triangular basins at high *Ra*.
2. Compare Large Eddy Simulation (LES) with WALE subgrid modeling to 2D DNS results.
3. Analyze temperature and flow fields to assess interactions between downslope currents and convective plumes.

METHOD

The numerical models for simulating thermal siphons in water bodies, particularly at high Rayleigh numbers (turbulent natural convection), fall into two categories:
1. Large Eddy Simulation (LES) models (2D), which require significant computational resources, and
2. Reynolds-Averaged Navier–Stokes (RANS) models, coupled with a turbulence model to account for turbulence effects.

In this study, Large Eddy Simulation (LES) is employed to investigate the quasi-steady state behavior of thermal siphons induced by surface cooling at high *Ra* numbers, using the WALE model to account for subgrid-scale turbulence and compares results with 2D DNS. Simulations use a time step Δt = 0.1 s (CFL condition) over 30,000 s. Boundary conditions (**Fig. 1**) are rigid, non-slip, adiabatic sides and bottom ($\partial T/\partial n$=0), a stress-free water surface with an applied thermal flux ($-\partial T/\partial y = B_0/(g\beta k)$, and an initially motionless water body at 293.15 K.

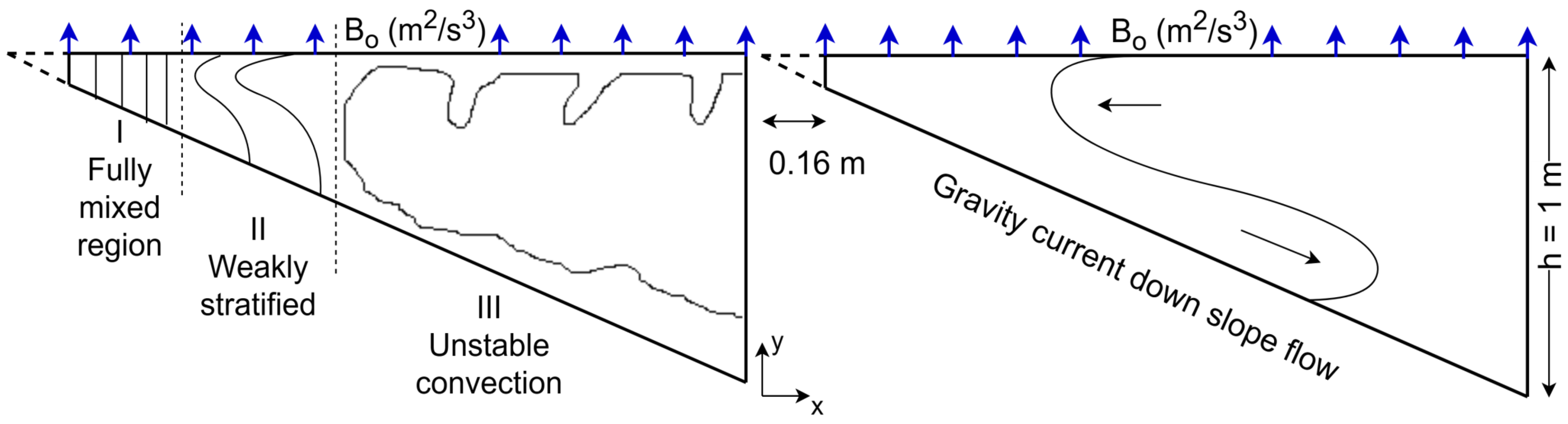

Figure 1. Characteristic flow regions (left) and conceptual model (right)

- The surface buoyancy outflow, B_0 (m^2/s^3) is defined as $B_0 = g\beta I_0/\rho_0 C_p$, where g: gravitational acceleration [m/s^2], β: thermal expansion coefficient [1/K]: surface cooling flux I_0 [W/m^2], ρ_0: fluid density [kg/m^3], Cp: water specific heat capacity at constant pressure [J/(kg·K)].
- The Rayleigh number, *Ra* is defined as $Ra = B_0 h^4/(\nu k^2)$, where: ν: kinematic viscosity [m^2/s], h: maximum water depth [m], k: thermal diffusivity [m^2/s].
- The Prandtl number, Pr is $Pr = \nu/k$ = 7.07 for water.
- Characteristic time scales were estimated following Ulloa et al. [3] and adapted for triangular water bodies for:
  - the onset of thermal instabilities at the free surface, $\tau_B \approx \sqrt{657.5}\,\sqrt{(\nu/B_0)}$. It decreases from 1813.1 s up to 57.3 s with increasing *Ra* from 10^{10} up to 10^{13}
  - the time for plumes to reach the bottom, $\tau_{RB} \approx h^{2/3}/B_0^{1/3}$. It decreases from 1710.0 s up to 171.0 s with increasing *Ra* number
  - the quasi-steady state, τ_{SS} ($\approx 2L^{2/3}/B_0^{1/3}$, L= total body length). It also decreases from 15873.7 s up to 1587.4 s with increasing *Ra* number.

RESULTS & DISCUSSION

The effect of *Ra* number on temperature and stream-function for the two highest *Ra* numbers studied is shown in the following figures. **Figure 2** shows the temperature for *Ra*=10^{11}. The DNS temperature field shows sharp plumes while the LES smooths gradients and underpredicts the peak by ~6%, slightly damping small-scale heat transfer. The DNS stream-function (**Fig. 3**) shows intricate vortices and secondary eddies, highlighting intense high-*Ra* turbulence. LES captures circulation, but misses smaller-scale features, with peak stream-function $\psi_{(DNS)}$ (=$\psi/\rho_0 q_c$) equal to 2.88 while is equal 2.82 for LES. The temperature T/T_0 (**Fig. 4**) fields at t/τ_{ss} = 5.04 show that the DNS exhibits finer thermal structures and larger temperature variations, while the LES appears smoother and warmer. The LES field spans a similar range ($0.983 \le T/T_0 \le 1.0$) with that of DNS ($0.982 \le T/T_0 \le 1.0$).

Figure 5 shows the large circulation pattern for the highest *Ra* number. Both DNS and LES capture the persistent large-scale circulation, though DNS reveals transient small-scale vortices mostly absent in LES.

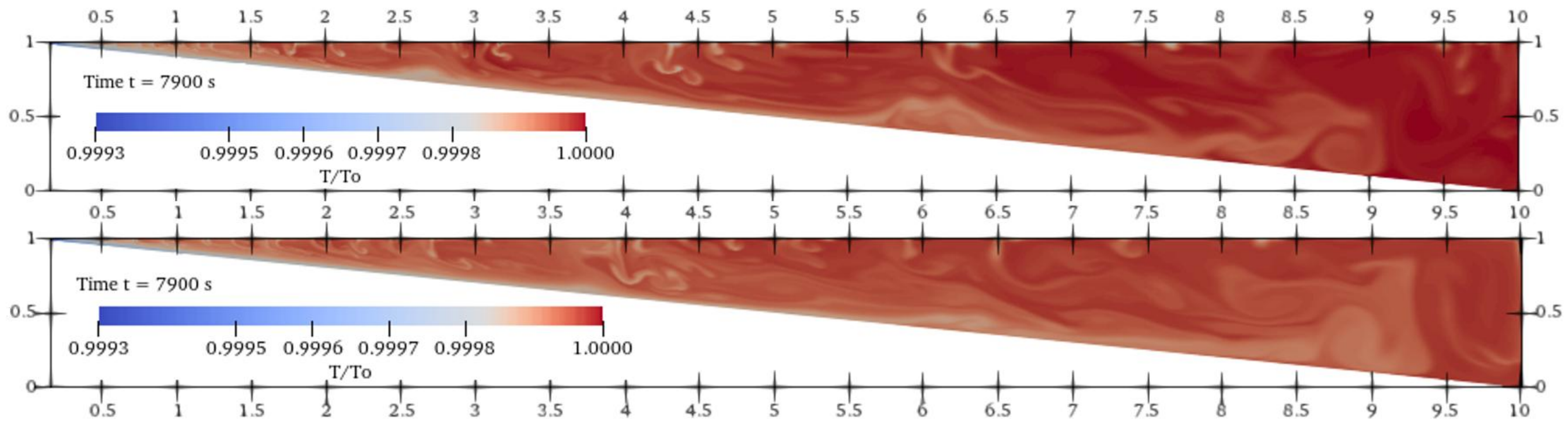

Figure 2. Temperature Ratio DNS (upper) & LES (lower) ($Ra = 10^{11}$, t/τ_{ss} = 1.07)

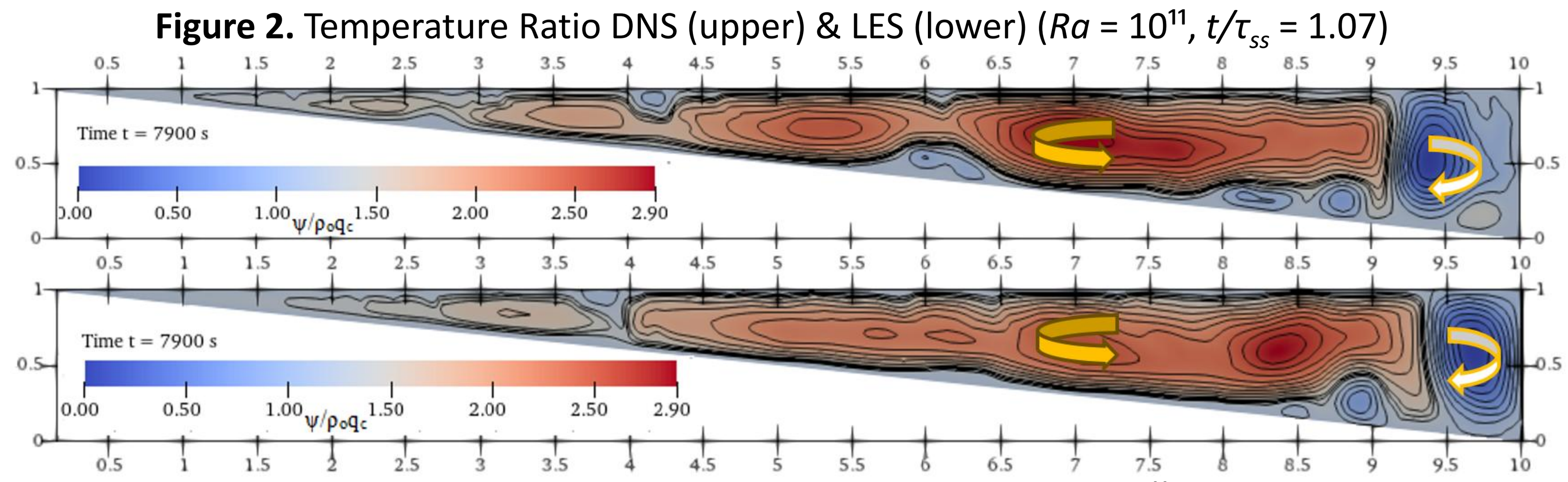

Figure 3. Stream-function DNS (upper) & LES (lower) ($Ra = 10^{11}$, t/τ_{ss} = 1.07)

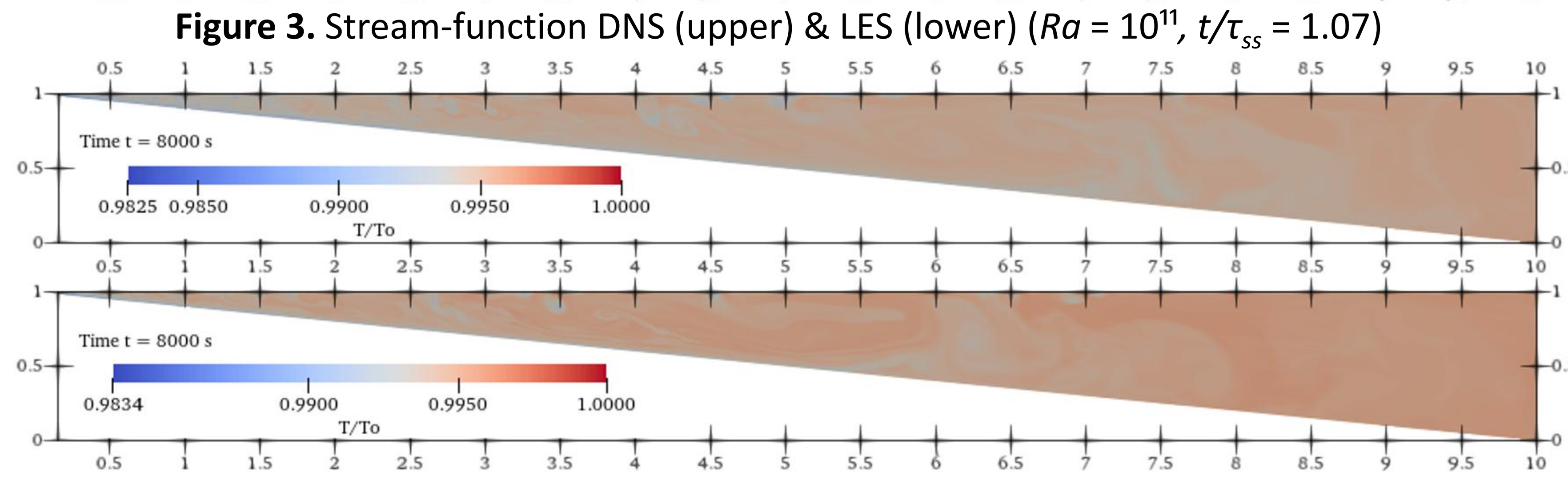

Figure 4. Temperature ratio DNS (upper) & LES (lower) ($Ra = 10^{13}$, t/τ_{ss} = 5.04)

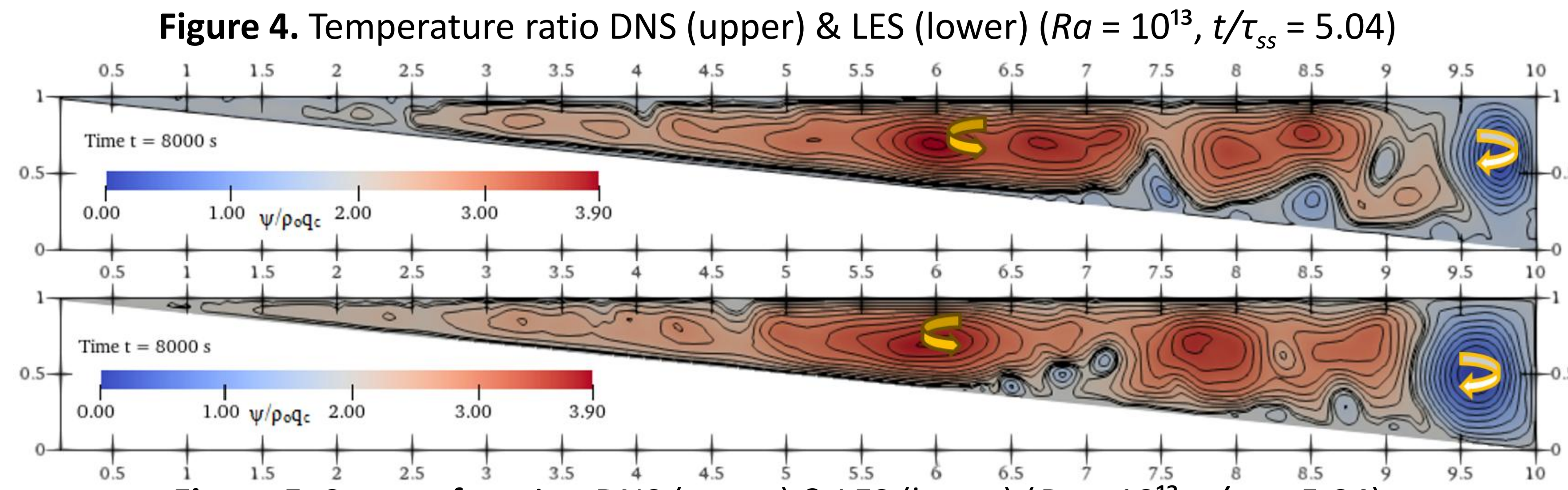

Figure 5. Stream-function DNS (upper) & LES (lower) ($Ra = 10^{13}$, t/τ_{ss} = 5.04)

CONCLUSION

For *Ra* = 10^{11} at t/τ_{ss} = 1.07 the DNS field exhibits sharp thermal plumes and fine-scale temperature fluctuations, capturing the small-scale turbulent structures. In contrast, the LES smooths these gradients due to its subgrid-scale modeling, which filters out the smallest scales of motion. Despite these differences, both DNS and LES accurately reproduce the gravity current responsible for flushing the bottom layer.
With increasing *Ra (Ra* = 10^{13}), Both cases exhibit similar large-scale flow structures and thermal patterns, indicating comparable overall mixing behavior. The DNS figure shows slightly cooler regions and sharper spatial gradients, reflected by the presence of more blue-toned areas.

FUTURE WORK / REFERENCES

Future work will extend simulations to 3D, explore LES-RANS hybrids, and investigate effects of uneven cooling, wind, and seasonal changes, as well as extreme *Ra* and long-term cooling to better understand turbulent thermal siphons.

[1] Mao, Y., Lei, C., & Patterson, J. C. (2010). Unsteady near-shore natural convection induced by surface cooling. Journal of Fluid Mechanics, 642, 213–233. https://doi.org/10.1017/S0022112009991765
[2] Papaioannou, V., & Prinos, P. (2023). Natural convection due to surface cooling in sloping water bodies with vegetation. *Journal of Hydraulic Research, 61*, 382–395. https://doi.org/10.1080/00221686.2023.2222094
[3] Ulloa, H. N., Ramón, C. L., Doda, T., Wüest, A., & Bouffard, D. (2022). Development of overturning circulation in sloping waterbodies due to surface cooling. Journal of Fluid Mechanics, 930, A18. https://doi.org/10.1017/jfm.2021.883
[4] Doda, T., Ulloa, H. N., Ramón, C. L., Wüest, A., & Bouffard, D. (2023). Penetrative convection modifies the dynamics of downslope gravity currents. Geophysical Research Letters, 50. https://doi.org/10.1029/2022GL100633